



Corrosion inhibition of X70 steel by thiourea-Zinc thiocyanate system in sodium chloride solution

A. Hamdi *, M.B. Taouti, D. Benbental

Laboratoire Physico-Chimie des Matériaux « LPCM », Université Amar Telidji BP 37G 03000 Laghouat Algeria

Received 14 July 2014; Revised 29 September 2014; Accepted 11 October 2014.

*Corresponding Author. E-mail: ah.hamdi@lagh-univ.dz ; Tel:(+213793383438)

Abstract

This study investigates corrosion inhibition of X70 mild steel using thiourea and zinc thiocyanate in a 3% NaCl solution with pH=5.5. The first part of the study compares the inhibitory effects of each component. For the 100ppm the inhibitory action of thiourea has not been clearly demonstrated, the electrochemical tests show that the inhibitory effect is more marked increasing by the concentration of zinc thiocyanate. The maximum inhibition efficiency obtained is 98.6% at 100ppm. The second part of this study presents the results obtained for two concentrations of thiourea mixed with zinc ions and zinc thiocyanate. Adsorption of thiourea and Zn(SCN)₂ on X70 steel surface was found to obey the Langmuir adsorption isotherm with a standard free energy of adsorption ΔG_{ads} -17.29 and -22.05 kJ/ mol respectively. The stationary polarization curves and electrochemical impedance spectroscopy (EIS) diagrams shows the mechanism of inhibition of the compounds studied.

Key words: corrosion, inhibition, thiourea, X 70 steel, Synergistic effects.

1. Introduction.

Mild steel is widely applied as constructional material in petrochemical industries due to its excellent mechanical properties and low cost. The breakdown of passive oxide films by aggressive anions such as Cl⁻ is frequently responsible for the failure of iron alloys in aqueous chloride solutions [1]. A variety of organic compounds containing heteroatom such as O, N, S and multiple bonds in their molecule are of particular interest as they give better inhibition efficiency than those containing N or S alone, as lone pair of electrons present on heteroatom are the important structural features that determine the adsorption of these molecules on the metal surface [2-4].

Thiourea has been studied for over four decades, because it inhibits steel corrosion in acidic media [5, 6]. Other researchers [7- 9] have also studied the mechanisms of adsorption of thiourea and its derivatives in acid medium. Iofa et al [10] found that the action of thiourea is caused by the chemisorption of sulfur atoms on the metal surface. Under the influence of the dipole created at the metal-solution interface, the sulfur moves onto the metal and the surface acquires a negative charge which adsorbs the organic cation. Lin et al [11] studied the effect of inhibiting the corrosion of steel by thiourea and Mg (II), Ca (II) and Al (III) ions in a solution of 3.5% NaCl and seawater. The effect of organic molecule associated with inorganic compounds on the corrosion of mild steel in acidic medium has been studied [12, 13].

In order to minimize the consumption of thiourea due to its environmental toxicity (Canadian Environmental Protection Act, 1999), in a first step we suggest a synergic action with thiourea and Zn(II) and in second step with thiourea and zinc thiocyanate.

2. Experimental

The material tested in this study is the low alloy X70 mild steel. The chemical composition of the material is given in table1. The quantitative and qualitative analyses of the samples were carried out by fluorescence of X-rays spectrometry (Philips XRF). The test media were 500 ml, 3 wt% NaCl prepared from reagent grade chemicals and bi-distilled water. When needed, HCl or NaOH, were added to adjust the pH which is monitored with a pH/temperature (°C) meter. All experiments were conducted at pH 5.5.

Table 1: Chemical components of the X70 steel used in the tests [14].

Element	Cr	Ni	Mn	Si	Nb	Co	Mo
(Wt %)	0.005	0.062	1.664	0.021	0.032	0.0159	0.0123
Cu	S	P	Ti	Al	C	V	Fe
0.3152	0.001	0.009	0.003	0.034	0.172	0.0665	rest

2.1. Potentiodynamic polarization measurements

For polarization studies, the X70 steel specimen was embedded in PVC holder using epoxy resin with an exposed area of 1.0 cm² as a working electrode. A platinum foil was used as an auxiliary electrode. The reference electrode was a saturated calomel electrode (SCE) coupled to a Luggin capillary whose tip was located between the working electrode and the auxiliary electrode. Before measurement, the electrode was immersed in a test solution at open circuit potential (OCP) for 30 min until a steady state was reached. All polarization measurements were performed using TACUSSEL model PGP201 galvanostat / potentiostat corrosion measurement system at room temperature under aerated conditions, the scanning rate was 0.5mVs⁻¹ and a sweep range from an initial potential of -1000 mV/SCE to a final potential of +200 mV/SCE.

2.2. EIS measurements

The electrochemical impedance spectroscopy measurements EIS were carried out using AC signals of amplitude 5 mV peak to peak at OCP (E_{corr}) in the frequency range from 10 kHz to 5 mHz, using TACUSSEL model PGZ401 at room temperature in an aerated solution. The working electrode has been prepared from a cylindrical rod of X70 steel to get an area exposed to solution of 1 cm², and immersed in the test solution for 120 min, to establish a steady state open circuit potential (OCP). EIS is recorded at open circuit potentials.

The charge transfer resistance values were obtained from the diameter of the semi circles of the Nyquist plots.

3. Results and discussion

3.1. Potentiodynamic polarization measurements

3.1.1. Effect of concentration

The polarization curves of X70 steel in 3% NaCl in the presence of various concentrations of Zn(SCN)₂ and thiourea are shown in Figure 1.

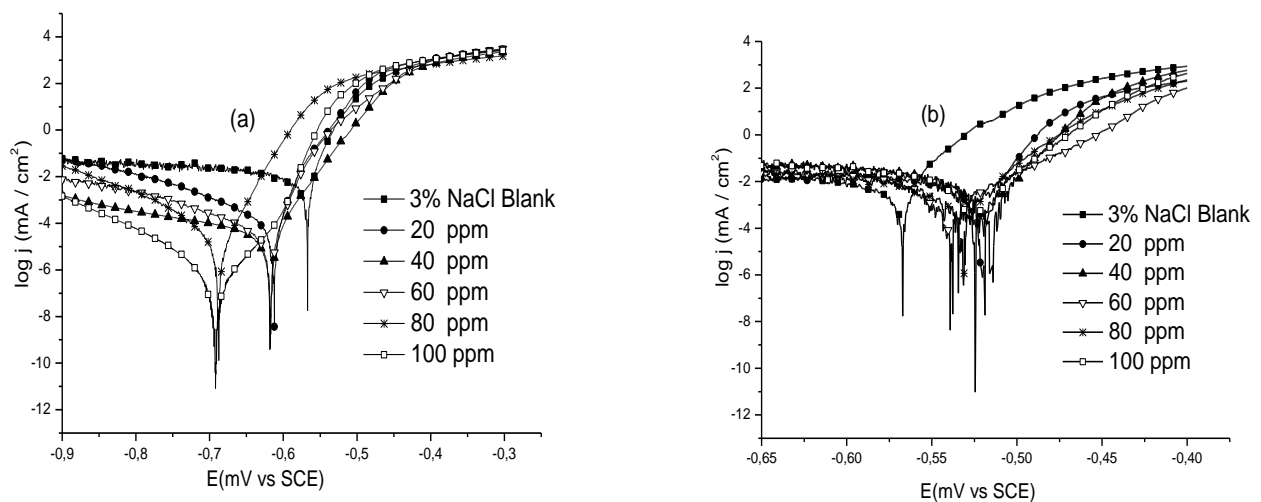


Figure 1: Polarization curves obtained from the X70 steel immersed in the solution without and with different inhibitors (a) Zn (SCN)₂, and (b) thiourea.

Table 2 illustrates the corresponding electrochemical parameters. The inhibition efficiency was calculated using the following equation:

$$IE(\%) = \frac{(j_{corr} - j'_{corr})}{j_{corr}} \times 100 \quad (1)$$

where j_{corr} and j'_{corr} are corrosion current densities without and with the inhibitor, respectively.

The inhibition efficiency increases with the presence of Zn(SCN)₂ and reached 98.6% for the 100 ppm, but increases slightly for thiourea is reaching 49% for the same concentration.

At high concentrations of Zn(SCN)₂, the values of cathodic slopes (β_c) which appear in Figure 1 (a) decrease, this indicates the influence of the Zn(SCN)₂ on the kinetics of hydrogen evolution. However with the addition of thiourea to 3%NaCl solution (Figure 1(b)) the values of β_c remain substantially unchanged. The reduction mechanism is not affected by the presence of the thiourea.

Table 2: Electrochemical parameters and inhibition efficiency at different inhibitors concentrations of X70 steel in 3%NaCl.

Concentration of inhibitor		$-E_{corr}/$ mV/SCE	$j_{corr}/$ $\mu A.cm^{-2}$	$\beta_a /$ mV.dec ⁻¹	$-\beta_c /$ mV.dec ⁻¹	CR / mm. Y ⁻¹	IE / %
Zn(SCN) ₂	Blank	567.6	86.70	34.1	224.6	1.01	0.00
	20 ppm	612.2	22.6	42.1	230.2	0.27	73.87
	40 ppm	618	8.7	52.7	228.9	0.10	89.94
	60 ppm	614.6	6.0	29.3	89.2	0.07	93.10
	80 ppm	688.1	4.5	40.3	61.9	0.05	94.87
	100 ppm	691.6	1.20	72.5	77.2	0.01	98.62
Thiourea	20 ppm	523.0	67.0	41.8	81.3	0.78	22.68
	40 ppm	519.1	53.4	31.9	77.5	0.62	38.46
	60 ppm	539.7	51.5	65.5	79.3	0.60	40.63
	80 ppm	549.9	49.5	30.5	52.7	0.58	42.90
	100 ppm	534.1	43.6	33.1	81.8	0.51	49.70

3.1.2. Study of the synergistic effect

The little inhibition efficiency recorded for thiourea alone encouraged us to study the synergistic inhibition between Z(II) ions or Zn(SCN)₂ and thiourea molecules in order to delay effectively X70 steel corrosion under these conditions.

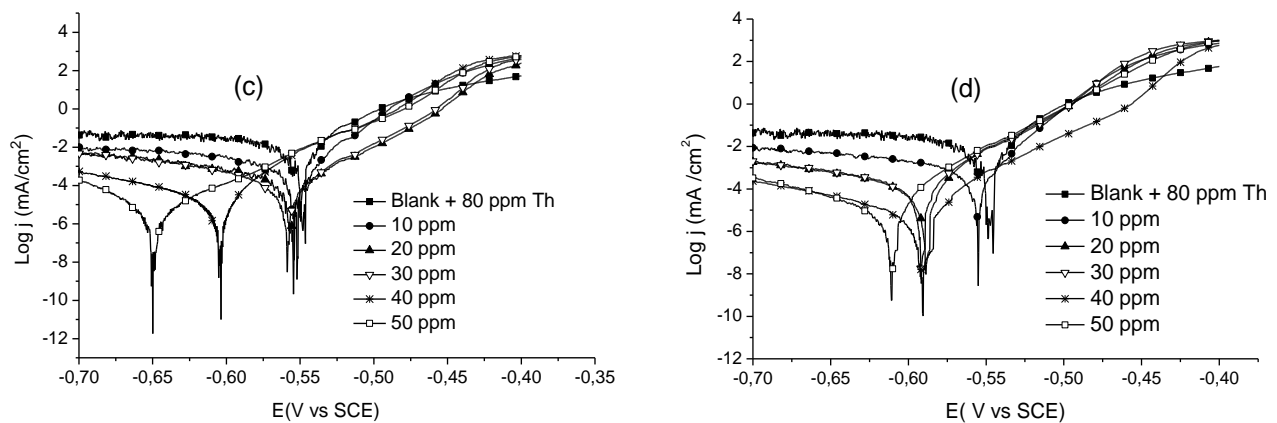


Figure 2: Polarization curves obtained for the X70 steel immersed in the 3% NaCl +80 ppm solution of thiourea without and with different concentration of (c) ZnCl₂ and (d) Zn (SCN)₂.

Table 3 shows the electrochemical corrosion kinetic parameters, corrosion current density j_{corr} obtained by extrapolation of the Tafel lines. It shows that the addition of the thiourea + Z(II) mixture to an aggressive media is accompanied by a decrease of the current densities, as compared to the blank solution and the solution with 80ppm thiourea.

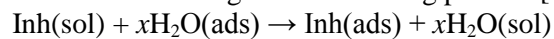
The addition of ZnCl₂ or Zn(SCN)₂ showed inhibition efficiency of 88.46% and 94.83% respectively. From the data of Table 3 it is seen that Zn(SCN)₂ would be considered as one of the most effective compounds for synergistic action with respect to the investigated two salts (ZnCl₂ and Zn(SCN)₂). The net increment of inhibition efficiency shows a synergistic effect of Zn(SCN)₂, and ZnCl₂ with thiourea. The synergistic effect depends on the type and concentration of anion (Cl⁻, SCN⁻) and zinc ion.

Table 3: The electrochemical parameters and inhibition efficiency of 80ppm thiourea, most for different concentrations of the Zn (II) ions and Zn (SCN)₂ for the corrosion of X70 steel obtained by polarization curves.

Concentration of inhibitor		-E _{corr} / mV/SCE	j _{corr} / μA.cm ⁻²	β _a / mV.dec ⁻¹	-β _c / mV.dec ⁻¹	CR / mm.Y ⁻¹	IE / %
80ppm thiourea + ZnCl ₂	0ppm	549.9	49.5	30.5	52.7	0.58	42.89
	10ppm	555.3	34.5	39	140.8	0.40	60.25
	20ppm	588.7	25.6	57.8	280.3	0.30	70.51
	30ppm	591.5	22.1	58.7	186.1	0.26	74.55
	40ppm	591	12	69.3	189.2	0.14	86.09
	50ppm	610.7	10.0	53.6	182.7	0.12	88.46
80ppm thiourea + Zn(SCN) ₂	10ppm	552.4	26.3	36.9	99.7	0.31	69.63
	20ppm	554.8	17.1	58.6	100.5	0.20	80.28
	30ppm	558.9	17.9	56.2	155.5	0.21	79.39
	40ppm	603.6	9.1	51.1	156.7	0.11	89.55
	50ppm	648.5	4.87	80.4	69.5	0.06	94.83

3.1.3. Adsorption isotherm

The adsorption of organic inhibitors at the metal/solution interface takes place through the replacement of water molecules by organic inhibitor molecules. According to the following process [15].



Values of surface coverage (θ) equation (2) corresponding to different concentrations of thiourea and zinc thiocyanate, were calculated using the Potentiodynamic polarization measurements at 303 K after 30 mn of immersion and were used to determine which isotherm best described the adsorption process. However, the best agreement was obtained using the Langmuir adsorption isotherm equation (3) as follows:

$$\theta = \frac{(j_{\text{corr}} - j'_{\text{corr}})}{j_{\text{corr}}} \quad (2)$$

$$\frac{C_i}{\theta} = \frac{1}{K_{\text{ads}}} + C_i \quad (3)$$

where C_i is the concentration of inhibitor and K_{ads} the adsorptive equilibrium constant.

Plots of C_i/θ against C_i yield straight lines as shown in Figure 3, and the linear regression parameters are listed in Table 4.

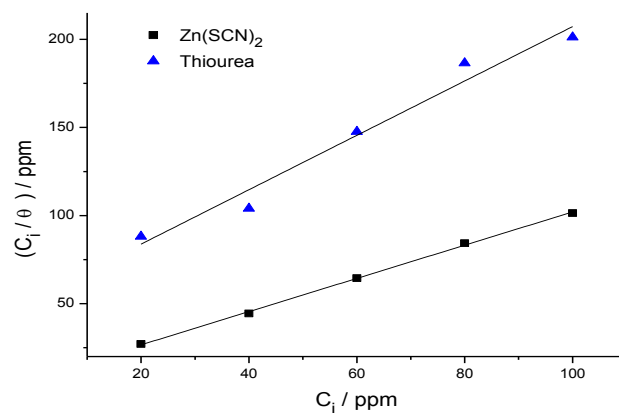


Figure 3: Curve fitting the corrosion of X70 steel in 3% NaCl in presence of different concentrations of thiourea and zinc thiocyanate to Langmuir adsorption isotherm at 25°C.

Both linear correlation coefficient (r) and slope are close to 1, indicating that the adsorption of the investigated inhibitors on the steel surface obeys the Langmuir adsorption. K_{ads} is related to the standard free energy of

adsorption ΔG_{ads} as shown in the following equation [16]:

$$K_{ads} = \frac{1}{55.5} \exp\left(\frac{-\Delta G_{ads}}{RT}\right) \quad (4)$$

values of ΔG_{ads} up to -20 kJ/ mol are consistent with the electrostatic interaction between the charged molecules and the charged metal (physical adsorption), while those more negative than -40 kJ /mol involve sharing or transfer of electrons from the inhibitor molecules to the metal surface to form a coordinate type of bond (chemisorption) [17,18]

The values of ΔG_{ads} of the two compounds presented in Table 4 are located in a range between -17.29 and 22.05 kJ/mol and this indicates physical adsorption. In addition to electrostatic interaction, there may be some other interactions.

Table 4: Adsorption equilibrium constant (K_{ads}) and standard free energy of adsorption (ΔG_{ads}) of the investigated surfactants for steel in a 3% NaCl solution at 25°C.

Inhibitors	correlation coef	Intercept	Slope	K_{ads}/M^{-1}	$\Delta G_{ads}/kJ.mol^{-1}$
Zn(SCN) ₂	0.99	7.80	116.31	128.30	-22.05
Thiourea	0.96	52.94	117.25	18.89	-17.29

3.2. Electrochemical impedance technique

The inhibition efficiency IE (%) was calculated using the charge transfer resistance as follows:

$$IE(\%) = \frac{(R'_{ct} - R_{ct})}{R'_{ct}} \times 100 \quad (5)$$

Where R_{ct} and R'_{ct} are the charge transfer resistance in the absence and presence of inhibitor, respectively. Nyquist and Bode impedance plots for the same experimental conditions are shown in Figure 4.

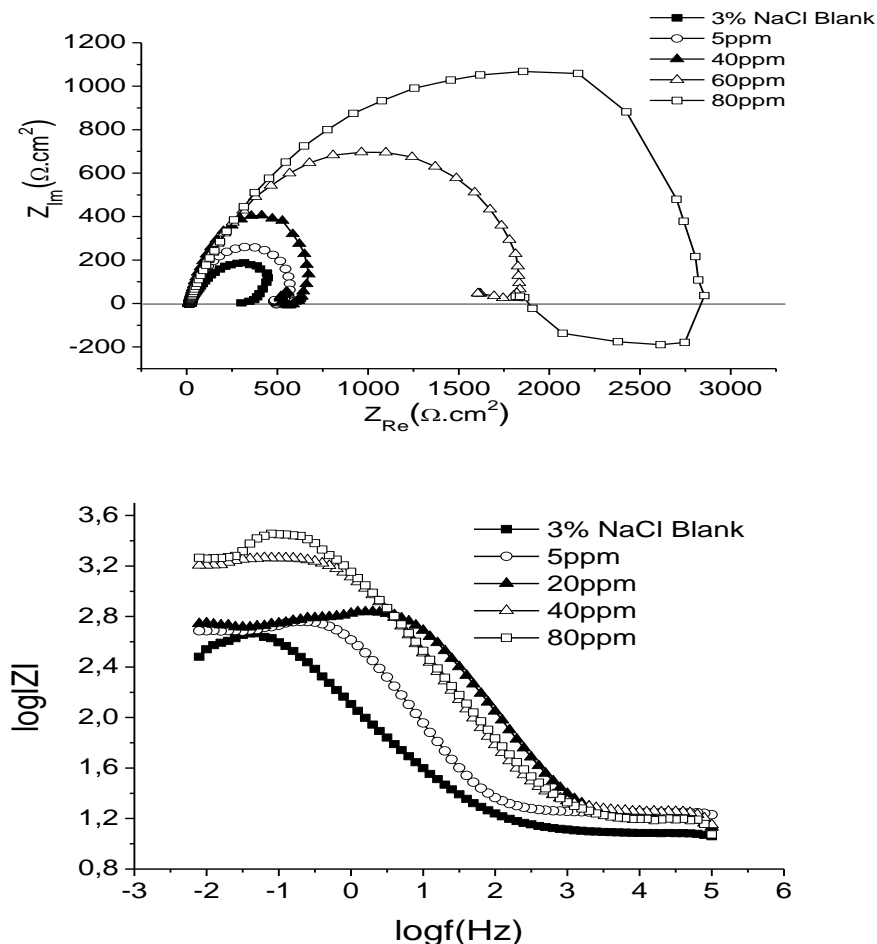


Figure 4: Impedance diagrams of X70 steel electrode in a 3%NaCl at E_{corr} in presence and absence of Zn(SCN)₂.

In all concentrations, $Zn(SCN)_2$ consist of a large capacitive loop at high frequencies (HF) and a small inductive one at low frequency values (LF). The semi-circle system for the 3% NaCl without inhibitor corresponds to the dissolution of the steel and the following formation of the complex, while the inductive loop is associated with an adsorption process. Migration, most probably in the presence of an electric field, leads precipitation and adsorption of ions.

With the addition of inhibitors at high frequencies a semicircle was formed, while at lower frequencies a second small inductive resistive semicircle appeared. The result suggests a passive state associated with the formation of a film inhibitor (semicircle at high frequency) while the low frequency semicircle charges transfer processes that are the salt of the film at local sites [19-21].

While the results suggest a reaction most likely controlled by the adsorption and migration of chloride ions to local sites forming a layer of salt, the presence of adsorbed inhibitors is indicated by an inductive loop at low frequency related to the local dissolution of steel in the presence of salt in the porous film [22-24].

Table 5: Efficiency and inhibitory parameters for electrochemical impedance measurements of X70 steel in a 3% NaCl medium with and without addition of $Zn(SCN)_2$.

Concentration of $Zn(SCN)_2$	$R_{ct}/\Omega.cm^2$	$C_{dl}/\mu F.cm^2$	-E / (mV/SCE)	IE/%
Blank	483.90	3289.20	572	0
5ppm	661.33	380.24	602	26.82
20ppm	1177.49	135.16	628	58.90
40ppm	1951.73	102.7	659	75.21
80ppm	3276	61.19	696	85.22

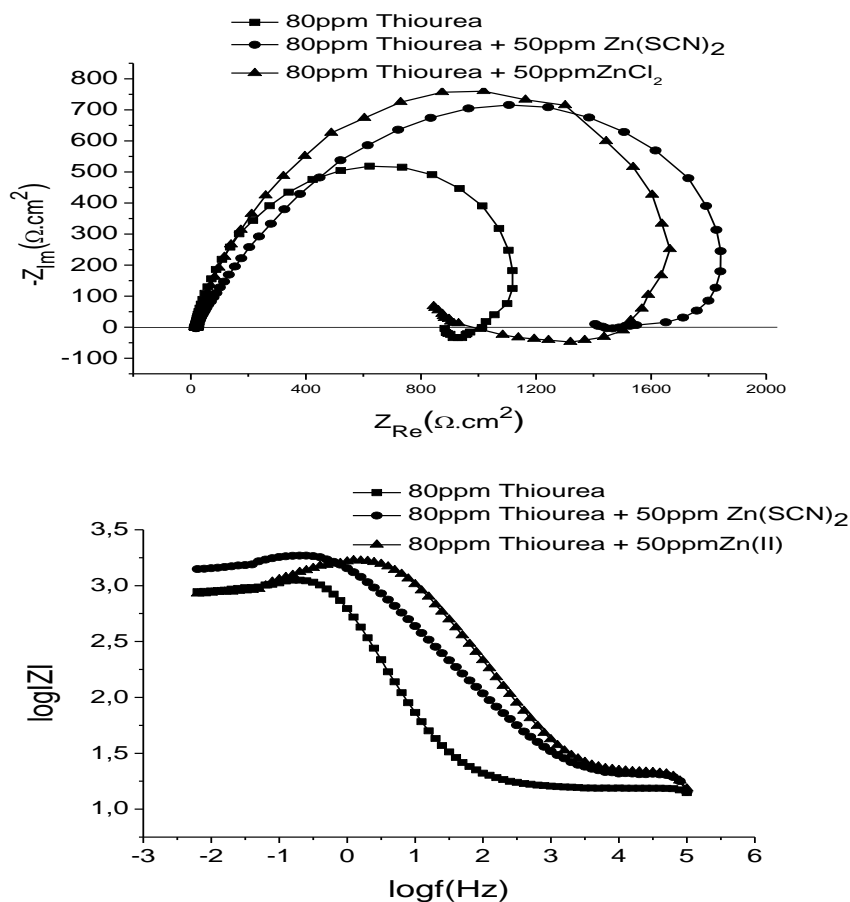


Figure 5: Impedance diagrams of X70 steel electrode in 3%NaCl at E_{corr} in presence 80ppm thiourea, 80ppm thiourea + $ZnCl_2$, and 80ppm thiourea+ $Zn(SCN)_2$.

Table 6: Inhibition efficiency and parameters related to electrochemical impedance measurements of X70 steel in 3% NaCl medium in presence 80ppm thiourea, 80ppm thiourea + ZnCl₂, and 80ppm thiourea + Zn(SCN)₂.

Concentration of inhibitor	R _{ct} /Ω.cm ²	C _{dl} /μF.cm ⁻²	E/mV	IE/%
80ppm thiourea	1354.92	148.2	-582	64.28
80 ppm Thiourée + 50ppm Zn(SCN) ₂	2145.29	74.5	-627	77.4
80ppm thiourée + 50ppm ZnCl ₂	2177.5	74.18	-640	77.77

We suggest the equivalent electrical circuit to describe the results of the EIS containing two times constants of relaxation. The resistance of the protective layer and the diffuse load capacity in it are not separated in this approximation, they are rather designed to be included in the circuit elements used [25,26].

It means that the circuit elements in Figure 6 will change with physical systems represented, but their significance has been validated by measurements and additional calculations. Figure 6 shows the equivalent circuit with simulated data obtained by the experimental curve.

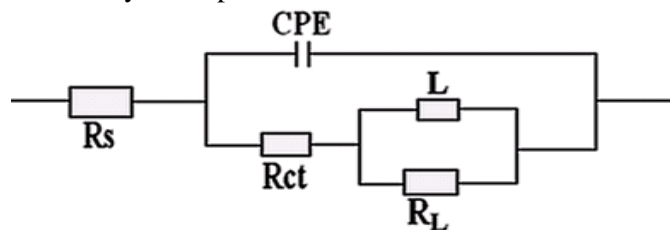


Figure 6: Equivalent circuits used to fit the EIS data of X70 steel in 3% NaCl + xppm inhibitor.

Where Rs: the resistance of the electrolyte, Rct: the resistance of the electrochemical reaction, R_L: the resistance of films inhibitor, L: inductance of films inhibitor, and CPE: the ability of the double layer.

The constant phase element, CPE, is presented in the circuit instead of a pure capacitor of the double layer to give a more accurate adjustment [27]. The resistance Rct represent a load transfer whose value is a measure of electron transfer through the surface and is inversely proportional to the corrosion rate [28]. The presence of the inductive loop RL - L can be attributed to the relaxation process obtained by adsorption species as Cl⁻_{ads} and H⁺_{ads} on the electrode surface [29, 30-32]. It may also be attributed to the re-dissolution of the passivity surface at low frequencies [33]. Thiocyanate ions adsorbed by the anodic site to formed a barrier between the metal surface and the corrosive solution. The zinc ions are precipitated on the cathode site as zinc hydroxide Zn (OH)₂ [34].

Conclusion

Following the above conducted studies, broad conclusions were drawn; the X-70 steel is not resistant for corrosion in 3% NaCl and at low acidity. In this case the low concentration of thiourea does not give us a good inhibitory efficiency. In contrast, the zinc salts have good efficiency because the zinc ions precipitate out in the form of hydroxide on the surface of the metal. The addition of zinc salts to thiourea enhanced the inhibition efficiency due to synergistic effect. The adsorption on X-70 steel surface by inhibitors molecules, obey Langmuir isotherm, the adsorption is a spontaneous endothermic process. According to the values of free energy of adsorption obtained we recommend Physical adsorption process.

References

1. McCafferty E., Hackerman N. *J. Electrochem. Soc.* 119 (1972) 999.
2. Donnelly B., Downie T. C., Gzeskowiak R., Hamburg H. R., Short D. *Corros. Sci.* 18 (1977) 109.
3. Thomas J. G. N. in: Proceedings of the 5th European Symposium on Corrosion Inhibitors, 5 SEIC, Ann. Univ. Ferrara, Italy, 1980, p. 453.
4. Benali O., Benmehdi H., Hasnaoui O., Selles C., Salghi R. *J. Mater. Environ. Sci.* 4 (1) (2013) 127.
5. Singh I. *Corrosion* 49 (1993) 473.
6. Awad ., Mohamed K. *J. Electroanal. Chem.* 567(2) (2004) 219.
7. Janssen M. J. *Spectrochim. Acta* 17 (1961) 475.

8. Shetty S. D., Shetty P., Nayak H. V. S. *J. Serb. Chem. Soc.* 71 (10) (2006) 1073.
9. Desai M. N., Thanki G. H., Gandhi M. H. *Anti. Corros. Method. M.* 15(7) (1968) 12.
10. Iofa Z. A., Batrakov V. V. *Electrochim. Acta* 9 (1964) 1645.
11. Lin J. C., Chang S. L., Lee S. L. *J. Appl. Electrochem.* 29 (1999) 911.
12. Antony S., Sahya R., Susai R. *J. Electrochem. Sci. Eng.* 2 (2012) 91.
13. Cenoui M., Dkhireche N., Kassou O., Ebn Touhami M., Tourir R., Dermaj A., Hajjaji N. *J. Mater. Environ. Sci.* 1 (2) (2010) 84.
14. Chaouche S. B., Lounis A., Nezzal G. *Int. J. of Microstructure and Materials Properties* 6 (2011) 526.
15. Xianghong Li., Shuduan D., Hui F., Taohong L. *Electrochim. Acta* 54 (2009) 4089.
16. Keles H., Keles M., Dehri I., Serindag O. *Mater. Chem. Phys.* 112 (2008) 173.
17. Alberty R., Silbey R. *Physical Chemistry, second ed, Wiley, New York, USA.*, 1997, p. 845.
18. Schapink F. W., Oudeman M., Leu K. W., Helle J. N. *J. Chem. Soc. Faraday Trans.* 56 (1960) 415.
19. MacDonald D. D. J. *Electrochem. Soc.* 125 (1978) 2063.
20. Khaled K. F. *J. Electrochem. Soc.*, 157(3) (2010) 116.
21. Zarrouk A., Zarrok H., Salghi R., Hammouti B., Bentiss F., Tourir R., Bouachrine M. *J. Mater. Environ. Sci.*, 4 (2) (2013) 177.
22. Noor E. A., Al-Moubaraki A. H. *Int. J. Electrochem. Sci.* 3 (2008) 806.
23. Luo J. L., Hileman O. E. J., Ives M. B. *Corros. Sci.* 35(1) (1993) 73.
24. Ferhat M., Benchettara A., Amara S. E., Najjar D. *J. Mater. Environ. Sci.* 5 (4) (2014) 1059.
25. Bressan J., Wiart R., Bressan J., Wiart R. *J. Appl. Electrochem.* 9 (1979) 615.
26. Dawson J. L., Ferreira M. G. S. *Corros. Sci.* 12 (1986) 1009.
27. Macdonald J. R., Potter Jr., Larry D. *Solid State Ionics* 24 (1987) 61.
28. Abdel-Gabar A. M., Abd-El-Nabey B. A., Sidahmed I. M., El-Zayady A. M., Saadawy M. *Corros. Sci.* 48 (2006) 2765.
29. Amin M. A., Abd El-Rehim S. S., El-Sherbini E. E. F., Bayyomi R. S. *Electrochim. Acta* 52 (2007) 3588.
30. Lenderrink H. J. W., Linden M. V. D., De Wit J. H. W. *Electrochim. Acta* 38(1993) 1989.
31. Kedam M., Mattos O. R., Takenouti H. *J. Electrochem. Soc.*, 128 (1981) 257.
32. Veloz M. A., González I. *Electrochim. Acta* 48 (2002) 135.
33. Sherif E. M., Park S. M. *Electrochim. Acta* 51 (2006) 1313.
34. Hassan H. H., Abdelghani E., Amin M. A. *Electrochim. Acta* 52 (2007) 6359.

(2015); <http://www.jmaterenvironsci.com>